Publications

# Current Sheet Flapping Motions in the Tailwind Flow of Magnetic Reconnection

Mingyu Wu
*University of Science and Technology of China*

Quanming Lu
*University of Science and Technology of China*

Martin Volwerk
*Austrian Academy of Sciences*

Zoltán Vörös
*Austrian Academy of Sciences*

Xuanye Ma
*University of Alaska, Fairbanks*, max@erau.edu

*See next page for additional authors*

## Scholarly Commons Citation

Wu, M., Lu, Q., Volwerk, M., Vörös, Z., Ma, X., & Wang, S. (2016). Current Sheet Flapping Motions in the Tailwind Flow of Magnetic Reconnection. *Journal of Geophysical Research: Space Physics, 121*(8). https://doi.org/10.1002/2016JA022819

Authors

Mingyu Wu, Quanming Lu, Martin Volwerk, Zoltán Vörös, Xuanye Ma, and Shui Wang

# RESEARCH ARTICLE

**Key Points:**
- The flapping motion of current sheet can also exist in the tailward flow
- The flapping motion is accompanied by magnetic turbulence
- The flapping motion occurs behind a large flux rope

**Correspondence to:**
Q. Lu,
qmlu@ustc.edu.cn

# Current sheet flapping motions in the tailward flow of magnetic reconnection

**Mingyu Wu[1,2], Quanming Lu[1,2], Martin Volwerk[3], Zoltán Vörös[3], Xuanye Ma[4], and Shui Wang[1]**

[1]CAS Key Laboratory of Geospace Environment, Department of Geophysics and Planetary Science, University of Science and Technology of China, Hefei, China, [2]Collaborative Innovation Center of Astronautical Science and Technology, Hefei, China, [3]Space Research Institute, Austrian Academy of Sciences, Graz, Austria, [4]Geophysical Institute, University of Alaska Fairbanks, Fairbanks, Alaska, USA

**Abstract** The feature and origin of current sheet flapping motions are one of most interesting issues of magnetospheric dynamics. In this paper we report the flapping motion of the current sheet detected in the tailward flow of a magnetic reconnection event on 7 February 2009. This flapping motion with frequency about 12 mHz was accompanied by magnetic turbulence. The observations by the tail-elongated fleet of five Time History of Events and Macroscale Interactions during Substorms probes indicate that these flapping oscillations were rather confined within the tailward flow than were due to a global process. This flapping motion could be due to the instability driven by the free energy associated with the ion temperature anisotropy in the tailward flow. Our observations indicate that the flapping motion in the tailward flow could have a different generation mechanism with that in the earthward flow.

## 1. Introduction

The Earth's cross-tail current sheet, also called as the neutral sheet [*Ness*, 1965], is a relatively narrow region in the center of the plasma sheet where the $x$ component of the magnetic field in the geocentric solar magneto-spheric (GSM) coordinate system has an abrupt directional change and the magnetic field intensity reaches a minimum. It is one of the key objects in magnetospheric physics. Previous observations find that the current sheet is a dynamic and turbulent region [*Valdivia et al.*, 2003]. It often flaps back and forth, which are recorded as multiple up-down crossings of the current sheet by the spacecraft [*Speiser and Ness*, 1967; *Toichi and Miyazaki*, 1976; *Lui et al.*, 1978; *Sergeev et al.*, 1998]. In the literatures these crossings are known as current sheet flapping motions [*Toichi and Miyazaki*, 1976; *Sharma et al.*, 2008].

Flapping motions manifest themselves as large-scale magnetic field variations with the amplitude of tens of nanotesla and a characteristic time of several to 10 min [*Sergeev et al.*, 1998; *Runov et al.*, 2005]. The spatial scale of flapping motions could be quite large. In an event observed on 5 August 2004, a current sheet flapping motion with the same phase was simultaneously observed by Double Star and Cluster which were about $5\,R_E$ apart along the Earth-Sun direction [*Zhang et al.*, 2005]. Furthermore, according to the statistical analysis, flapping motions tend to be triggered in the central part of the tail by some impulsive processes and then propagate toward the tail flanks as kink-like waves [*Sergeev et al.*, 2004]. The propagation speed of flapping motions is usually in the range 30–70 km/s [*Runov et al.*, 2005]. Analyses revealed that the flapping motion is due to current sheet corrugation. *Petrukovich et al.* [2006] have pointed out that the deformation of the current sheet has two types: the slip type and bend type. The slip-type deformation means that the magnetic flux tubes just shift vertically relative to their neighbors, but the normal direction of the flux tubes does not change, while the bend-type deformation means that the magnetic flux tubes rotate and then lead to the change of the normal direction of the flux tubes. With the measurements from Cluster, *Shen et al.* [2008] have studied several flapping events and found that the magnetic flux tubes deformation in the flapping current sheet is the slip type. Based on the observation results, *Rong et al.* [2010] constructed a simple magnetic model and tried to provide the physical interpretation for the slip-type deformation.

The generation mechanism of flapping motions is not well established yet. But previous studies have pointed out that flapping motions are related to the change of solar wind conditions [*Sergeev et al.*, 2008; *Vörös et al.*, 2014] or some internal processes in the magnetotail [*Davey et al.*, 2012]. Several theoretical models have been proposed to describe flapping motions. *Golovchanskaya and Maltsev* [2005] suggested that the ballooning-type mode excited by the existence of the curved magnetic field in the current sheet can lead to flapping

motions. *Zelenyi et al.* [2009] demonstrated that the drift-kink instability due to the relative drift of ions and electrons [*Daughton*, 1999] can be the driver of flapping motions. Recently, a new model of the magnetic double-gradient mode was proposed to indicate that flapping motions are caused by the gradient of the normal magnetic field component along the current sheet [*Erkaev et al.*, 2008, 2009; *Korovinskiy et al.*, 2013; *Sitnov et al.*, 2014]. In this model, the source for flapping motions is associated with bursty bulk flows (BBFs) [*Angelopoulos et al.*, 1992; *Baumjohann et al.*, 1990] originated from the reconnection region [*Erkaev et al.*, 2009; *Sitnov et al.*, 2014].

BBFs generated during magnetic reconnection are considered to be the main driver of magnetic fluctuations in the current sheet [*Volwerk et al.*, 2004; *Vörös*, 2011]. By analyzing a current sheet flapping event observed by Time History of Events and Macroscale Interactions during Substorms (THEMIS), *Gabrielse et al.* [2008] suggested that flapping motions are linked to BBFs. Statistical results demonstrated that the occurrence rate of flapping motions is similar to that of BBFs, and both of them have a peak in the central part of magnetotail [*Sergeev et al.*, 2006]. These observation results revealed that flapping motions could be closely related to BBFs.

During magnetic reconnection, high-speed tailward flows can also be generated as BBFs. While moving tailward, the high-speed tailward flows tend to evolve toward more relaxed states without interaction with the strong dipole-like field of the Earth, providing a clearer image of the steady physics processes, which can shed more light on the waves in magnetic reconnection. It is beneficial for us to understand waves in magnetic reconnection. However, until now flapping motion events in tailward flows have not been explored. In this paper, we investigate an anomalous magnetic reconnection event observed by the THEMIS mission on 7 February 2009, where the current sheet flapping motion is only identified in tailward flows, and observational evidence suggests that the flapping motion can be driven by some local processes in the tailward flow of magnetic reconnection.

## 2. Data and Instruments

The THEMIS mission has five spacecraft (probes) with identical instrumentation on board [*Angelopoulos*, 2008]. On 7 February 2009, the apogees of THEMIS probes are located in the magnetotail. The five spacecraft lie almost on one line, and THB is the outmost probe in the magnetotail. This configuration is suitable for simultaneous observations of large-scale waves or structures at different locations in the magnetotail. In this paper, we use the 4 Hz magnetic field data obtained by the fluxgate magnetometer (FGM) [*Auster et al.*, 2008]. FGM also supplies high-resolution data with 128 Hz. The 3 s spin average plasma data with energies less than 30 keV are obtained from the electrostatic analyzers (ESAs) [*McFadden et al.*, 2008]. All spacecraft data used in this paper are in the geocentric solar magnetospheric (GSM) coordinate system unless noted otherwise.

## 3. Observations

At the time 04:01:00 UT on 7 February 2009, THB was located at about $[-30.6, -1.7, -4.2]$ $R_E$ in the plasma sheet. Figure 1 shows the observational results of THB. From the top to the bottom panels, they are the three components of magnetic field $B_x$, $B_y$, $B_z$, the total magnetic field $|B|$, the $x$ component of the bulk flow velocity $v_{ix}$, the ion temperature $T_i$, the ion density $n_i$, the electron energy flux spectrograms, and the ion energy flux spectrograms. In Figure 1, the resolution of the magnetic field data is 0.25 s, while the particle data has a time resolution of 3 s. As shown in Figure 1e, THB was initially located in the tailward flow (the high-speed flow with the negative $v_{ix}$). At about 04:18:00 UT as marked by the vertical red line, the sign of $v_{ix}$ of the high-speed flow measured by THB turned from negative to positive. The reversal of the sign of $v_{ix}$ is accompanied by a simultaneous reversal of the sign of $B_z$. The sign of $B_z$ is negative in the tailward flow, while it is positive in the earthward flow (the high-speed flow with positive $v_{ix}$). The simultaneous reversals of $B_z$ and $v_{ix}$ reveal that THB observed a magnetic reconnection event. This magnetic reconnection event was also investigated by previous works [*Oka et al.*, 2011; *Sitnov et al.*, 2014]. In this magnetic reconnection event, $v_{ix}$ of the tailward flow reaches up to 630 km/s, which is much higher than that of the earthward flow. The tailward flow is hotter and more tenuous than the earthward flow. The ion temperature in the tailward flow is often higher than 2 keV, which is several times higher than that in the earthward flow. The ion density in the tailward flow is several times lower than that in the earthward flow. According to the theoretical model of magnetotail reconnection, such as two-dimensional (2-D) particle-in-cell reconnection simulations starting with Harris current
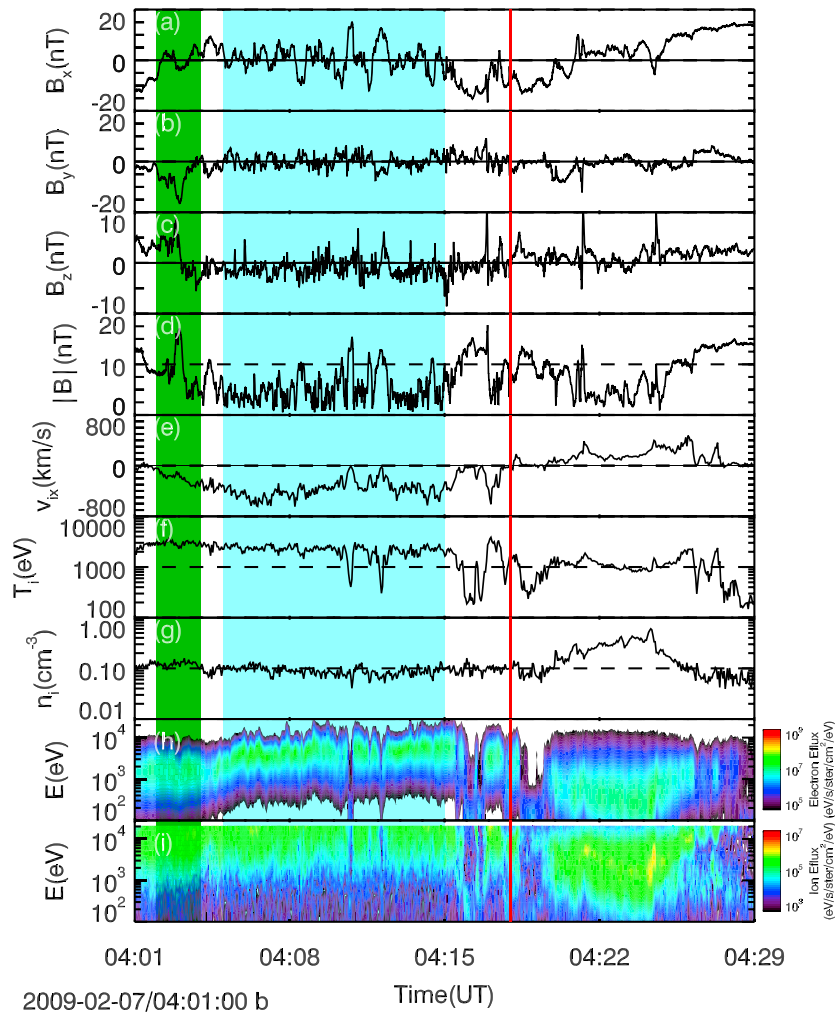
**Figure 1.** THB observations: the three components of magnetic field (a) $B_x$, (b) $B_y$, and (c) $B_z$, (d) the total magnetic field $|B|$, (e) the $x$ component of the bulk flow velocity $v_{ix}$, (f) the ion temperature $T_i$, (g) the ion density $n_i$, (h) the electron energy flux spectrograms, and (i) the ion energy flux spectrograms. The electron and ion energy flux is in the unit of eV/(s sr cm$^2$ eV). The time interval 04:02–04:04 UT is marked by the green color, while the time interval 04:04–04:15 UT is marked by the light blue color. The vertical red line indicates the simultaneous reversal of $B_z$ and $v_{ix}$.
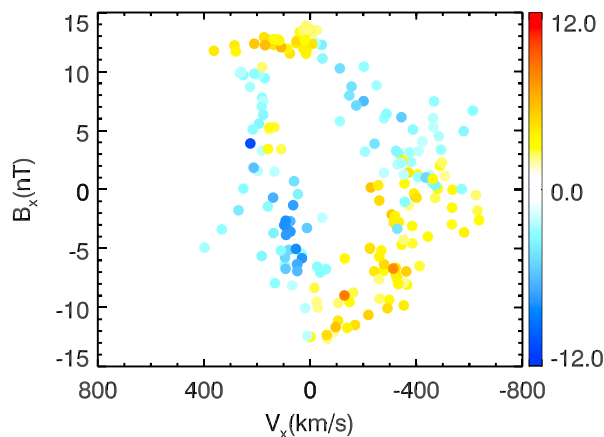


**Figure 2.** The Hall magnetic field $B_y$ as a function of $B_x$ and $v_{ix}$.

sheets, particles in the earthward and tailward flows both originated from the lobe region [e.g., *Goldman et al.*, 2015]. So there is a possibility that some processes occurred in the outflow region leading to the differences of ion density and temperature in the earthward and tailward flows.

We now examine the magnetic field signatures of this event in more detail. Figure 2 shows the distribution of the $B_y$ component. The $B_y$ component has a quadrupole structure, which fits the prediction of antiparallel Hall reconnection well [*Eastwood*
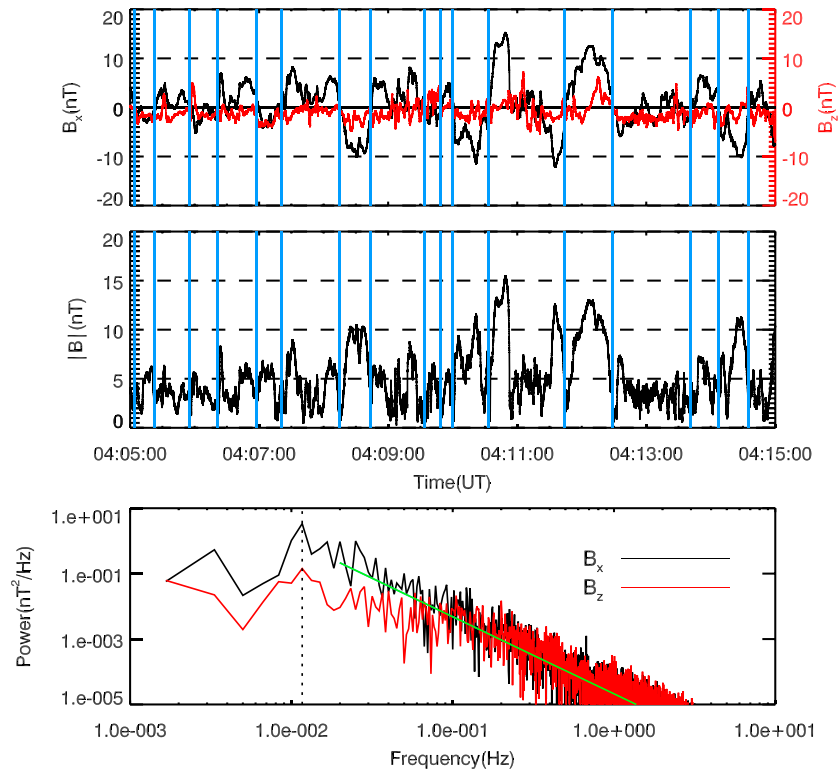
**Figure 3.** (top) The 128 Hz magnetic field components $B_x$ (black line) and $B_z$ (red line), (middle) the total magnetic field $|B|$, and (bottom) the power spectra of $B_x$ (black line) and $B_z$ (red line). The vertical blue lines indicate the crossings of current sheet. The vertical dashed line is the highest peak of $B_x$ and $B_z$. The spectral power of $B_x$ is fitted with respect to frequency over the interval [0.2, 1] Hz to obtain the spectral index and shown as the green line.

*et al.*, 2010]. The quadrupole Hall magnetic field $B_y$ also supports that the spacecraft THB have encountered a magnetic reconnection event. Besides, in the tailward and earthward flows, there are some flux ropes which are identified by the bipolar structure of $B_z$ and a strong core field $B_y$ at the center of the bipolar $B_z$ signature. During the time interval 04:02:00–04:04:00 UT marked by the green color in Figure 1, a clear bipolar $B_z$ variation (see Figure 1c) from 8.6 nT to $-5.4$ nT is detected. Both the $y$ component (Figure 1b) and magnitude (Figure 1d) of magnetic field have an obvious peak near the reversal point of $B_z$. These magnetic signatures suggest a possibility that a flux rope was passed by the spacecraft. This flux rope is located in the leading edge of the tailward flow. The maximum and minimum values of $B_z$ are detected at 04:02:51 UT and 04:03:46 UT. During the time interval from 04:02:51 UT to 04:03:46 UT, the averaged flow speed is about $-300$ km/s. Therefore, the diameter of the center of this flux rope is about 2.6 $R_E$, which are about 23 local ion inertial lengths. Inside this flux rope there is an isolated population of ~1 keV electrons, which is considered as the plasmoid/flux rope signature [e.g., *Zong et al.*, 2004; *Sormakov and Sergeev*, 2008].

Strong magnetic fluctuations can be observed in the high-speed flows, especially in the tailward flow. Now we focused on the magnetic field variations in the tailward flow during the time interval 04:05 UT–04:15 UT which is marked by the light blue color. Such time interval is behind the flux rope marked by the green color. In this 10 min, the position of THB changes about [0.01, 0.59, 0.07] $R_E$, which means that the spacecraft moves slowly along the $y$ direction. We use the data with the high resolution (128 Hz) to investigate the features of the magnetic field variations. Figure 3 (top) shows the magnetic field components $B_x$ (black line) and $B_z$ (red line), and Figure 3 (middle) gives the total magnetic field $|B|$. As shown in Figure 3, the spacecraft is initially located in the current sheet indicated by a small $B_x$. At about 04:05:04 UT, the reversal of $B_x$ from positive to negative indicates that the spacecraft THB crosses the current sheet from north to south. After this crossing, multiple crossings of the current sheet were detected. Every crossing is marked by a vertical blue line. It can be found that all crossings satisfy the definition of current sheet: the $B_x = 0$ and the magnetic field intensity $|B|$ reaches a minimum. In Figure 3 (top), we can find that the average value of $B_z$ is about $-2$ nT. However,

**Table 1.** Current Sheet Crossings on 7 February 2009 by THB[a]

| Center Time | $\Delta t$ | MVA Normal in GSM | $\lambda_2/\lambda_3$ | $k$ |
|---|---|---|---|---|
| 04:06:58 | 20 | 0.05, 0.57, 0.82 | 8.5 | −1 |
| 04:07:21 | 20 | 0.33, 0.67, 0.66 | 2.3 | 1 |
| 04:08:15 | 20 | 0.09, 0.62, 0.78 | 1.6 | −1 |
| 04:08:44 | 20 | 0.02, −0.15, −0.99 | 1.9 | 1 |
| 04:09:34 | 20 | −0.21, −0.18, −0.96 | 2.3 | −1 |
| 04:09:49 | 20 | −0.38, −0.08, −0.92 | 3.8 | 1 |
| 04:10:00 | 20 | 0.22, 0.60, 0.77 | 2.7 | −1 |
| 04:10:33 | 20 | 0.06, 0.05, −1.00 | 7.8 | −1 |
| 04:11:44 | 20 | −0.08, 0.02, 0.99 | 2.7 | 1 |
| 04:12:29 | 20 | 0.06, 0.55, 0.83 | 5.0 | −1 |

[a]From the left column to the right column, there are center time which is the time when THB is crossing the CS center ($B_x \sim 0$), the adopted time interval for MVA which is centered at the center time, the MVA normal in GSM, the ratio of eigenvalues $\lambda_2/\lambda_3$, and the value of $k$.

$B_z$ can have a positive value when $B_x$ is positive. Additionally, both $B_x$ and $B_z$ have high-frequency magnetic fluctuations. We employ the Fourier transform method to investigate the magnetic wave activity. Figure 3 (bottom) shows the power spectra of $B_x$ (black line) and $B_z$ (red line). The highest peak in the spectrum of $B_x$ marked by the vertical dashed line is located at about 12 mHz. The highest peak in the spectrum of $B_z$ is also located at the same frequency. It indicates that $B_x$ and $B_z$ have the same dominant period. This could be caused by the vertical flapping motion of the current sheet. If the amplitude of $B_z$ decreases monotonically with the distance from the neutral sheet, in the vertical flapping the amplitude of $B_x$ will increase/decrease with the decrease/increase of the amplitude of $B_z$. Therefore, the oscillations of $B_x$ and $B_z$ would have the same dominant period. The power spectra of $B_x$ and $B_z$ with the frequency higher than 0.2 Hz have a turbulent wave spectrum. In the power spectrum of $B_x$, a linear fit of the power density is made over the frequency range [0.2, 1] Hz. We use this linear fit to obtain the spectral index. The results of this linear fit are shown by the green line. The spectral index is about 2.6. Such magnetic fluctuations in the frequency range [0.2, 1] Hz are the magnetic turbulence.

*Rong et al.* [2015] developed a single-point technique to diagnose the flapping type. With single-point magnetic field measurements, the normal direction $\mathbf{n} = (n_x, n_y, n_z)$ of the current sheet can be estimated by minimum variance analysis (MVA) method. Besides, they designate the value of $B_x$ from negative to positive as $\Delta B_x > 0$ while the value from positive to negative as $\Delta B_x < 0$. Then, the parameter $k$ can be defined as $k = \mathrm{sign}(n_y \times n_z) \times \mathrm{sign}(\Delta B_x)$. If $k$ changes sign for neighboring crossings of the current sheet, the flapping motion is an oscillation which does not propagate toward tail flanks. In the previous literatures, this type of flapping motion is named as "the steady flapping" [e.g., *Rong et al.*, 2015]. In contrast, if $k$ has the same value for each crossing, the flapping motion is a kink-like wave which can propagate along the $y$ direction. In this event, we calculate the normal direction of the current sheet at each crossing. In Figure 3 we can notice that there are full of high-frequency oscillations of $B_x$. Therefore, in our calculations a low-pass filter is used to eliminate the high-frequency noise. The normal direction and $k$ of each crossing during the time interval 04:06:50–04:13:00 UT are given in Table. 1. In this time interval 04:06:50–04:13:00 UT, the results of MVA do not strongly depend on the time interval where we choose to calculate the normal direction at each crossing. As shown in Table. 1, $k$ always changes its sign at neighboring crossings. According to *Rong et al.* [2015], it indicates that the flapping motion in our event is just a vertical oscillation and does not propagate as kink-like waves. The observed flapping in the tailward flow is the steady flapping. However, there is a deviation at 04:10:33. At this crossing of the current sheet at 04:10:33, we can find $n_z >> n_y \sim 0$ which means that the current sheet surface is almost horizontal. In such case, $\mathrm{sign}(n_y \times n_z)$ is not reliable and the value of $k$ has a significant deviation.

Figure 4 shows interplanetary magnetic field (IMF) and solar wind conditions recorded by OMNI during 02:30–04:30 UT on 7 February 2009 with 1 min time resolution. From the top to the bottom panels, they are three components of magnetic field $B_x$, $B_y$, and $B_z$, three components of the solar wind bulk velocity, ion density $n_i$, the ion temperature $T_i$, the solar wind ram pressure, and the location of the bow shock nose. In the OMNI data set, the bow shock model of *Farris and Russell* [1994] with the magnetopause model of *Shue et al.* [1997] is used to determine the bow shock nose location. The solar wind flow aberration associated with Earth's ~30 km/s orbital motion about the Sun in bow shock nose location determination is also included. Around 03:41 UT, there is an interface in the solar wind (marked by the vertical dashed line), and almost all the parameters have a sharp jump near this interface. The amplitudes of $B_x$, $B_y$, and $B_z$ increase about 1 nT. The $V_x$ of the solar wind decreases about 5 km/s, while both $V_y$ and $V_z$ increase about 10 km/s. The flow
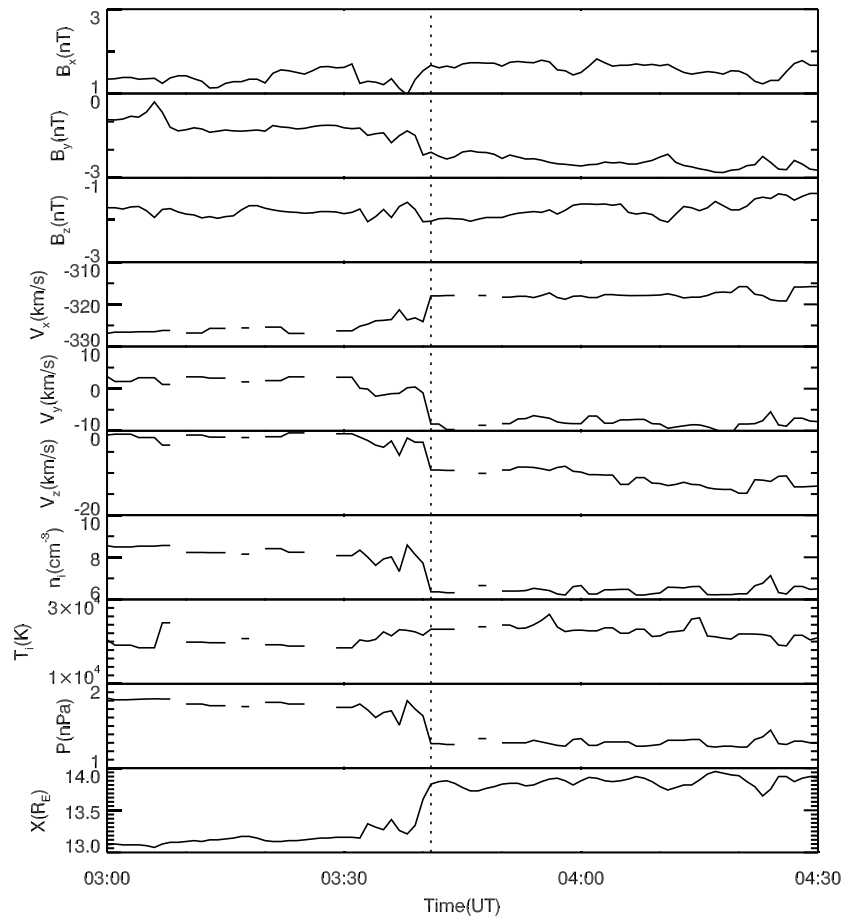
**Figure 4.** IMF and solar wind conditions recorded by OMNI during 02:30–04:30 on 7 February 2009. From the top to the bottom panels, they are three components of magnetic field $B_x$, $B_y$, and $B_z$, three components of the solar wind bulk velocity, ion density $n_i$, the ion temperature $T_i$, the flow pressure, and the location of the bow shock nose.

pressure decreases, and the position of bow shock nose changes about 0.8 $R_E$. After 03:41 UT, bow shock nose is located at about 13.9 $R_E$. This interface does not contain any magnetic discontinuities, but the solar wind changes its direction in the interface. One can find that the value of $V_z$ increases from ~1 to ~10 km/s. Previous simulation results suggested that changes in $V_z$ of the solar wind can lead to significant variations of the shape and location of the current sheet in the middle and deep parts of magnetotail [*Sergeev et al.*, 2008]. The simulation and observation results suggested that the current sheet has a complicated temporal response to the changes of the solar wind direction which can cause a shift of the current sheet in the *z* direction within the first 10–15 min, and it would take a much longer time (exceeding 0.5–2.5 h) to reach a new equilibrium [*Vörös et al.*, 2014]. According to this theory, the change of the solar wind direction near the interface can lead a global flapping motion of current sheet in the magnetotail. In our event, $V_x$ in the solar wind is about −320 km/s. The interface needs to take about 15 min to arrive at the location of THB in the magnetotail. Then the change of the solar wind direction can influence the current sheet. According to the previous theory, at least the global flapping motion can persist until the time 04:26 UT.

As shown in Figures 5a1 and 5a2, during the time interval 04:05–04:15 all five THEMIS probes were located in the plasma sheet, and they were roughly aligned along the x direction over more than 20 $R_E$. Using conjunctions with five THEMIS probes, we can have simultaneous observations at about −10, −17, and −31 $R_E$. Such observations can help us to confirm whether the flapping motion is a global or local process. Figures 5b1–5b5 present the results of $B_x$ observed by THEMIS probes. We find that the other four spacecraft did not observe the similar oscillations of the current sheet as THB. From 04:08 to 04:13 the other four spacecraft observed quiet plasma sheet, while at the same time the flapping motion observed by THB had the
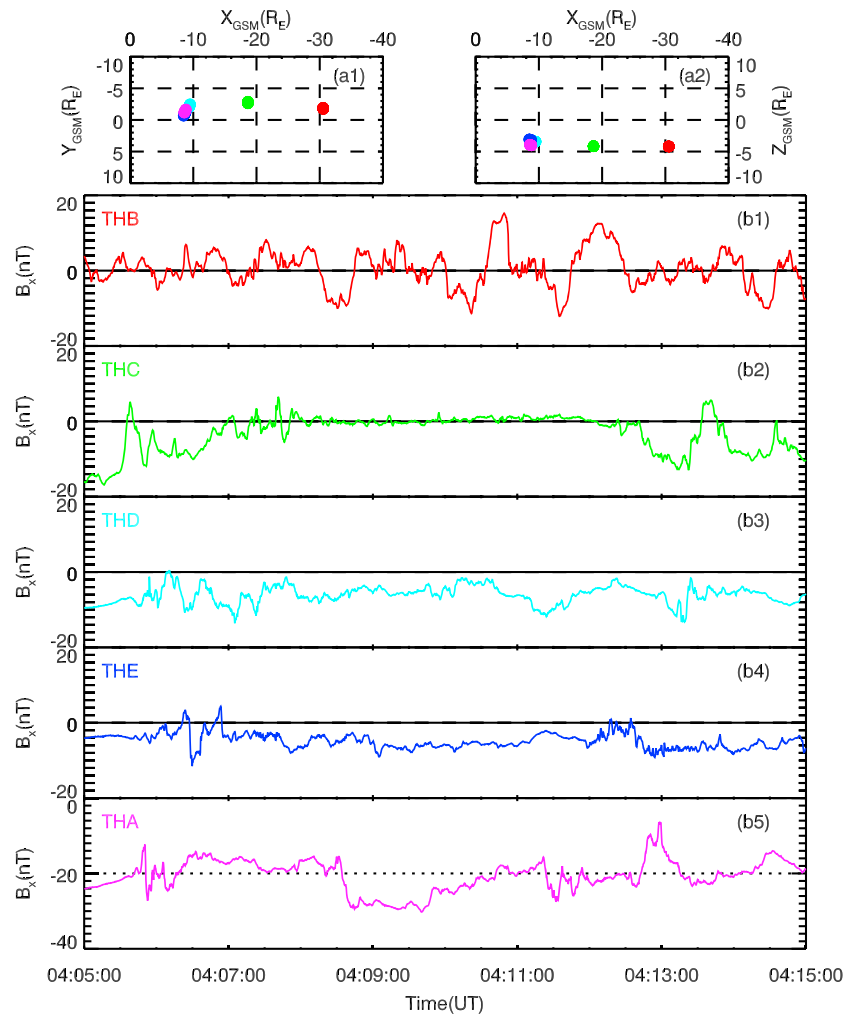
**Figure 5.** The location of five THEMIS probes in (a1) *X-Y* plane and (a2) *X-Z* plane, (b1) $B_x$ observed by THB (red) during the time 04:05–04:15 UT, (b2) $B_x$ observed by THC (green), (b3) $B_x$ observed by THD (cyan), (b4) $B_x$ observed by THE (blue), and (b5) $B_x$ observed by THA (pink).

largest amplitude. It indicates that in our event, the flapping motion of the current sheet in the tailward flow was a local process rather than a global process caused by the change of solar wind conditions. Additionally, if the change of the solar wind direction can lead to flapping motions, the change of the solar wind direction near the interface can also influence the current sheet during the time interval when the earthward flow driven by magnetic reconnection is observed (at least in the time interval before 04:26 UT). However, the spacecraft did not detect such flapping motions in the earthward flow. It also supports the conclusion that the flapping motion in the tailward flow is a localized phenomenon, which could be driven by some localized processes.

As outlined above, the tailward flow leading by a flux rope is observed. During the time interval behind the flux rope, a flapping motion of the current sheet is observed in this tailward flow. With the observation results we try to give a possible generation mechanism of the flapping motion in the tailward flow. The ion temperature in the tailward flow is shown in Figure 6. Figure 6 (top) gives the ion perpendicular temperature $T_{perp}$ (blue line) and the ion parallel temperature $T_{para}$ (green line). Figure 6 (bottom) gives the ratio of $T_{para}/T_{perp}$. We can find that most of the time the parallel temperature $T_{para}$ is higher than the perpendicular temperature $T_{perp}$ in the tailward flow. Ions have an anisotropic distribution in the tialward flow. The anisotropic tailward flow contains the free energy which can drive the instability. With 2-D hybrid simulations, *Arzner and Scholer* [2001] found that the post plasmoid/flux rope current sheet has a flapping motion.
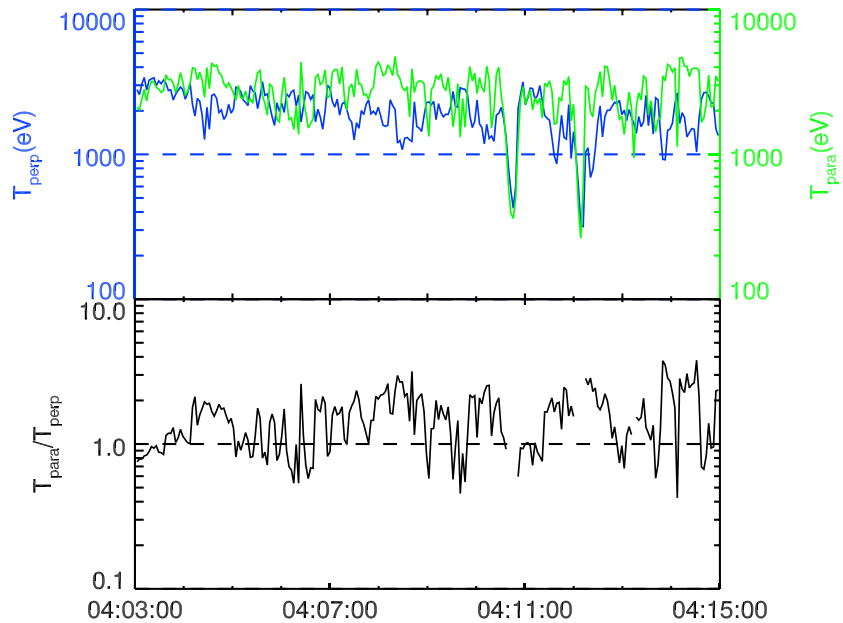
**Figure 6.** (top) The two components of ion temperature and (bottom) the ratio of $T_{para}/T_{perp}$.

They constructed an anisotropic fluid model to explain the generation of the flapping motion. The flapping motion in their simulations is due to an instability driven by an anisotropic flow in the post plasmoid/flux rope plasma sheet. Such instability is neither of pure Kelvin-Helmholtz mode nor of homogeneous firehose mode but can be explained by a combination of the two effects within a simple anisotropic flow. Based on their model, in our event the free energy contained by the anisotropic tailward flow could generate the instability which then leads to the observed flapping motion.

Figure 7 shows the sketch of a possible configuration of this magnetic reconnection event. The blue line is the magnetic field line, and the red lines show the positions of the current sheet. In this magnetic reconnection event, a large flux rope was produced and then propagated tailward. In the plasma sheet behind this flux rope, the instability which was driven by the free energy of ion temperature anisotropy in the tailward flow can develop. Then this instability caused the observed flapping of the current sheet in the tailward flow. The observed flapping is a vertical oscillation without propagation along the $y$ direction. Based on the
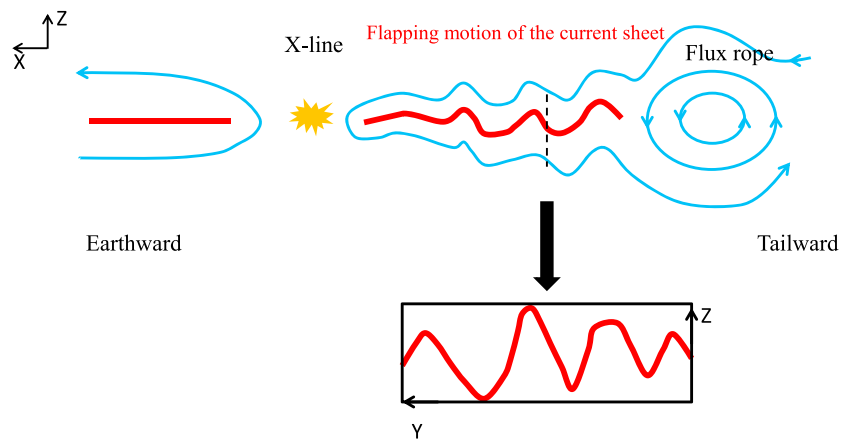


**Figure 7.** The sketch of this magnetic reconnection event. The blue line is the magnetic field line, and the black lines show the positions of the current sheet. A flux rope is in the tailward flow, and the current sheet behind the flux rope has a flapping motion. A rough sketch of the flapping current sheet in the $y$-$z$ plane at the position marked by the vertical dashed line is also shown in the black box.

computed normal directions shown in Table 1, the normal orientations of the flapping mainly varied in the *y-z* plane. In Figure 7, the rough sketch of the flapping current sheet in the *y-z* plane at the position marked by the vertical dashed line is shown in the black box. This type of flapping is named as the steady flapping in previous literatures.

## 4. Discussion and Conclusions

In summary, a magnetic reconnection event is identified by the simultaneous reversal of $B_z$ and $v_{ix}$ in the magnetotail. The Hall magnetic field $B_y$ in this event fits the quadrupole structure well, especially in the tailward flow. A flapping motion of the current sheet was observed in the tailward flow of magnetic reconnection, and the frequency of the flapping motion is about 12 mHz. This flapping motion is a vertical oscillation without propagation along the *y* direction. Additionally, this flapping motion is accompanied by magnetic turbulence. By the conjunction observations with five THEMIS probes, the flapping motion in the tailward flow is not a global process. The generation of this flapping motion could be due the instability driven by free energy associated with the ion temperature anisotropy in the tailward flow.

The current sheet in the magnetotail seems to be a turbulent region. Previous theoretical work and observations have demonstrated that the current sheet exhibits stochastic properties over a broad range of spatial and temporal scales [*Uritsky et al.*, 2002; *Valdivia et al.*, 2003]. Turbulence can play an important role in the multiscale energy conversion. In our event, the flapping motion is accompanied by a stochastic component which is considered to be magnetic turbulence. The tailward flow is probably the main driver of the observed turbulence in the current sheet. The spectral index of the magnetic turbulence is 2.6, which is the same as the spectral index observed in the earthward flow [*Volwerk et al.*, 2004; *Vörös et al.*, 2004]. This high index implies that the turbulence is quasi-two dimensional, but not strict. The flapping motion of current sheet could lead to some three-dimensional effects. Besides, the observed time interval of tailward flow could also make sense on the high index. Usually, the time interval of high-speed flows in the magnetotail is much shorter than that of solar wind flows. The shorter intervals can lead to that the inertial range of turbulence with the small spectral index ~1.6 observed in the solar wind cannot be seen in the magnetotail, unless there are longer interval of data available in the magnetotail [*Vörös et al.*, 2007]. The flapping motion and the related turbulence indicate that there is a multiscale energy dissipation process in the tailward flow of magnetic reconnection.

The previous models of the magnetic double-gradient mode [*Erkaev et al.*, 2008, 2009] suggested that the current sheet becomes unstable in the region where $B_z$ decreases locally toward Earth. The recent particle-in-cell simulations [*Sitnov et al.*, 2014] further showed that BBFs leading by a dipolarization front can produce the local earthward decrease of $B_z$ and then trigger the flapping motion. However, this model cannot well describe the flapping motion in the tailward flow of magnetic reconnection. *Arzner and Scholer* [2001] have proposed an anisotropic fluid model to explain the flapping motion behind a plasmoid/flux rope in the tailward flow. They found that ions in the tailward flow can be accelerated in the current sheet behind a tailward propagated plasmoid/flux rope and then these ions can have an anisotropic distribution. The combination of the anisotropy of ions and the shear between the high-speed tailward flow in the current sheet and the lobe plasma can lead to the instability. This instability can cause the flapping of the current sheet. In our event, the flapping motion occurs during the time interval behind a flux rope, and the tailward flow also has anisotropy. Our observations fit predictions of the anisotropic fluid model proposed by *Arzner and Scholer* [2001] well. It indicates that the flapping motion in the tailward flow can have a different generation mechanism with that in the earthward flow.

## References

Angelopoulos, V. (2008), The THEMIS mission, *Space Sci. Rev.*, *141*, 5–34, doi:10.1007/s11214-008-9336-1.
Angelopoulos, V., W. Baumjohann, C. F. Kennel, F. V. Coroniti, M. G. Kivelson, R. Pellat, R. J. Walker, H. Lühr, and G. Paschmann (1992), Bursty Bulk flows in the inner central plasma sheet, *J. Geophys. Res.*, *97*, 4027–4039, doi:10.1029/91JA02701.
Arzner, K., and M. Scholer (2001), Kinetic structures of the post plasmoid plasma sheet during magnetotail reconnection, *J. Geophys. Res.*, *106*, 3827–3844, doi:10.1029/2000JA000179.
Auster, H. U., et al. (2008), The THEMIS fluxgate magnetometer, *Space Sci. Rev.*, *141*, 235–264, doi:10.1007/s11214-008-9365-9.
Baumjohann, W., G. Paschmann, and H. Lühr (1990), Characteristics of high-speed ion flows in the plasma sheet, *J. Geophys. Res.*, *95*, 3801–3809, doi:10.1029/JA095iA04p03801.
Daughton, W. (1999), Two-fluid theory of the drift kink instability, *J. Geophys. Res.*, *104*, 28,701, doi:10.1029/1999JA900388.
Davey, E. A., M. Lester, S. E. Milan, and R. C. Fear (2012), Storm and substorm effects on magnetotail current sheet motion, *J. Geophys. Res.*, *117*, A02202, doi:10.1029/2011JA017112.

Eastwood, J. P., T. D. Phan, M. Øieroset, and M. A. Shay (2010), Average properties of the magnetic reconnection ion diffusion region in the Earth's magnetotail: The 2001–2005 Cluster observations and comparison with simulations, *J. Geophys. Res.*, *115*, A08215, doi:10.1029/2009JA014962.

Erkaev, N. V., V. S. Semenov, and H. K. Biernat (2008), Magnetic double gradient mechanism for flapping oscillations of a current sheet, *Geophys. Res. Lett.*, *35*, L02111, doi:10.1029/2007GL032277.

Erkaev, N. V., V. S. Semenov, I. V. Kubyshkin, M. V. Kubyshkina, and H. K. Biernat (2009), MHD model of the flapping motions in the magnetotail current sheet, *J. Geophys. Res.*, *114*, A03206, doi:10.1029/2008JA013728.

Farris, M. H., and C. T. Russell (1994), Determining the standoff distance of the bow shock: Mach number dependence and use of models, *J. Geophys. Res.*, *99*, 17,681–17,689, doi:10.1029/94JA01020.

Gabrielse, C., V. Angelopoulos, A. Runov, L. Kepko, K. H. Glassmeier, H. U. Auster, J. McFadden, C. W. Carlson, and D. Larson (2008), Propagation characteristics of plasma sheet oscillations during a small storm, *Geophys. Res. Lett.*, *35*, L17S13, doi:10.1029/2008GL033664.

Goldman, M. V., D. L. Newman, and G. Lapenta (2015), What can we learn about magnetotail reconnection from 2D PIC Harris-sheet simulations?, *Space Sci. Rev.*, doi:10.1007/s11214-015-0154-y.

Golovchanskaya, I. V., and Y. P. Maltsev (2005), On the identification of plasma sheet flapping waves observed by Cluster, *Geophys. Res. Lett.*, *32*, L02102, doi:10.1029/2004GL021552.

Korovinskiy, D. B., A. Divin, N. V. Erkaev, V. V. Ivanova, I. B. Ivanov, V. S. Semenov, G. Lapenta, S. Markidis, H. K. Biernat, and M. Zellinger (2013), MHD modeling of the double-gradient (kink) magnetic instability, *J. Geophys. Res. Space Physics*, *118*, 1146–1158, doi:10.1002/jgra.50206.

Lui, A. T. Y., C.-I. Meng, and S.-I. Akasofu (1978), Wavy nature of the magnetotail neutral sheet, *Geophys. Res. Lett.*, *5*, 279–282, doi:10.1029/GL005i004p00279.

McFadden, J. P., C. W. Carlson, D. Larson, J. Bonnell, F. Mozer, V. Angelopoulos, K.-H. Glassmeier, and U. Auster (2008), THEMIS ESA first science results and performance issues, *Space Sci. Rev.*, *141*, 477–508, doi:10.1007/s11214-008-9433-1.

Ness, N. F. (1965), The Earth's magnetic tail, *J. Geophys. Res.*, *70*, 2989, doi:10.1029/JZ070i013p02989.

Oka, M., T.-D. Phan, J. P. Eastwood, V. Angelopoulos, N. A. Murphy, M. Øieroset, Y. Miyashita, M. Fujimoto, J. McFadden, and D. Larson (2011), Magnetic reconnection X-line retreat associated with dipolarization of the Earth's magnetosphere, *Geophys. Res. Lett.*, *38*, L20105, doi:10.1029/2011GL049350.

Petrukovich, A. A., T. L. Zhang, W. Baumjohann, R. Nakamura, A. Runov, A. Balogh, and C. Carr (2006), Oscillatory magnetic flux tube slippage in the plasma sheet, *Ann. Geophys.*, *24*(6), 1695–1704, doi:10.5194/angeo-24-1695-2006.

Rong, Z. J., C. Shen, A. A. Petrukovich, W. X. Wan, and Z. X. Liu (2010), The analytic properties of the flapping current sheets in the Earth magnetotail, *Planet. Space Sci.*, *58*(10), 1215–1229, doi:10.1016/j.pss.2010.04.016.

Rong, Z. J., S. Barabash, G. Stenberg, Y. Futaana, T. L. Zhang, W. X. Wan, Y. Wei, and X.-D. Wang (2015), Technique for diagnosing the flapping motion of magnetotail current sheets based on single-point magnetic field analysis, *J. Geophys. Res. Space Physics*, *120*, 3462–3474, doi:10.1002/2014JA020973.

Runov, A., et al. (2005), Electric current and magnetic field geometry in flapping magnetotail current sheets, *Ann. Geophys.*, *23*, 1391–1403, doi:10.5194/angeo-23-1391-2005.

Sergeev, V., V. Angelopoulos, C. Carlson, and P. Sutcliffe (1998), Current sheet measurements within a flapping plasma sheet, *J. Geophys. Res.*, *103*, 9177–9188, doi:10.1029/97JA02093.

Sergeev, V., A. Runov, W. Baumjohann, R. Nakamura, T. L. Zhang, A. Balogh, P. Louarn, J.-A. Sauvaud, and H. Reme (2004), Orientation and propagation of current sheet oscillations, *Geophys. Res. Lett.*, *31*, L05807, doi:10.1029/2003GL019346.

Sergeev, V. A., D. A. Sormakov, S. V. Apatenkov, W. Baumjohann, R. Nakamura, A. V. Runov, T. Mukai, and T. Nagai (2006), Survey of large-amplitude flapping motions in the midtail current sheet, *Ann. Geophys.*, *24*, 2015–2024, doi:10.5194/angeo-24-2015-2006.

Sergeev, V. A., N. A. Tsyganenko, and V. Angelopoulos (2008), Dynamical response of the magnetotail to changes of the solar wind direction: An MHD modeling perspective, *Ann. Geophys.*, *26*, 2395–2402, doi:10.5194/angeo-26-2395-2008.

Sharma, A. V., et al. (2008), Transient and localized processes in the magnetotail: A review, *Ann. Geophys.*, *26*, 955–1006, doi:10.5194/angeo-26-955-2008.

Shen, C., Z. J. Rong, X. Li, M. Dunlop, Z. X. Liu, H. V. Malova, E. Lucek, and C. Carr (2008), Magnetic configurations of tail tilted current sheet, *Ann. Geophys.*, *26*, 3525–3543, doi:10.5194/angeo-26-3525-2008.

Shue, J.-H., J. K. Chao, H. C. Fu, C. T. Russell, P. Song, K. K. Khurana, and H. J. Singer (1997), A new functional form to study the solar wind control of the magnetopause size and shape, *J. Geophys. Res.*, *102*, 9497–9511, doi:10.1029/97JA00196.

Sitnov, M. I., V. G. Merkin, M. Swisdak, T. Motoba, N. Buzulukova, T. E. Moore, B. H. Mauk, and S. Ohtani (2014), Magnetic reconnection, buoyancy and flapping motions in magnetotail explosions, *J. Geophys. Res. Space Physics*, *119*, 7151–7168, doi:10.1002/2014JA020205.

Sormakov, D., and V. Sergeev (2008), Topology of magnetic flux ropes in the magnetospheric plasma sheet as measured by the Geotail spacecraft, *Cosmic Res.*, *46*, 387–391, doi:10.1134/S0010952508050031.

Speiser, T. W., and N. F. Ness (1967), The neutral sheet in the geomagnetic tail: Its motion, equivalent currents, and field line reconnection through it, *J. Geophys. Res.*, *72*, 131, doi:10.1029/JZ072i001p00131.

Toichi, T., and T. Miyazaki (1976), Flapping motions of the tail plasma sheet induced by the interplanetary magnetic field variations, *Planet. Space Sci.*, *24*, 147, doi:10.1016/0032-0633(76)90102-1.

Uritsky, V., A. J. Klimas, and D. Vassiliadis (2002), Multiscale dynamics and robust critical scaling in a continuum current sheet model, *Phys. Rev. E*, *65*, 046113, doi:10.1103/PhysRevE.65.046113.

Valdivia, D., A. Klimas, D. Vassiliadis, V. Uritsky, and J. Takalo (2003), Self-organization in current sheet model, *Space Sci. Rev.*, *107*, 515–522, doi:10.1023/A:1025518527128.

Volwerk, M., et al. (2004), Multi-scale analysis of turbulence in the Earth's current sheet, *Ann. Geophys.*, *22*, 2525–2533, doi:10.5194/angeo-22-2525-2004.

Vörös, Z. (2011), Magnetic reconnection associated fluctuations in the deep magnetotail: ARTEMIS results, *Nonlinear Process. Geophys.*, *18*, 861–869, doi:10.5194/npg-18-861-2011.

Vörös, Z., et al. (2004), Magnetic turbulence in the plasma sheet, *J. Geophys. Res.*, *109*, A11215, doi:10.1029/2004JA010404.

Vörös, Z., W. Baumjohann, R. Nakamura, A. Runov, M. Volwerk, Y. Asano, D. Jankovicova, E. A. Lucek, and H. Reme (2007), Spectral scaling in the turbulent Earth's plasma sheet revisited, *Nonlinear Process. Geophys.*, *14*, 535–541, doi:10.5194/npg-14-535-2007.

Vörös, Z., G. Facskó, M. Khodachenko, I. Honkonen, P. Janhunen, and M. Palmroth (2014), Windsock memory COnditioned RAM (CO-RAM) pressure effect: Forced reconnection in the Earth's magnetotail, *J. Geophys. Res. Space Physics*, *119*, 6273–6293, doi:10.1002/2014JA019857.

Zelenyi, L. M., A. V. Artemyev, A. A. Petrukovich, R. Nakamura, H. V. Malova, and V. Y. Popov (2009), Low frequency eigenmodes of thin anisotropic current sheets and Cluster observations, *Ann. Geophys.*, *27*, 861–868, doi:10.5194/angeo-27-861-2009.

Zhang, T. L., et al. (2005), Double Star/Cluster observation of neutral sheet oscillations on 5 August 2004, *Ann. Geophys.*, *23*, 2909–2914, doi:10.5194/angeo-23-2909-2005.

Zong, Q.-G., et al. (2004), Cluster observations of earthward flowing plasmoid in the tail, *Geophys. Res. Lett.*, *31*, L18803, doi:10.1029/2004GL020692.